POST-DRYOUT HEAT TRANSFER TO R12 IN A CIRCULAR 90-DEG-TUBE-BENDS

G. Lautenschlager, F. Mayinger

Lehrstuhl A für Thermodynamik
Technische Universität München, FRG

ABSTRACT

A study of post-dryout heat transfer to Freon 12 in an electrically heated circular 90-degree-tube-bend is reported. Experimental results at different mass flux densities (400 - 2000 kg/m²s), critical pressure ratios (0.225 - 0.675) and heat flux densities (2 - 8 W/cm²) are presented. When dispersed flow enters a bend separation of liquid from vapour phase occurs due to different inertial forces which leads to an increase in heat transfer at the outer and a decrease at the inner wall of the bend. The traverse motion of the droplets towards the outer wall mainly depends on drop size, velocity and density ratio of the two phases at the bend inlet. Rewetting of the outer wall is improved by decreasing pressure ratios and increasing mass flux densities. Due to a circumferential secondary flow induced by the centrifugal force and superimposed on the main flow, heat transfer at the inner side of the bend strongly depends on the conditions at the outer side. Therefore after an axial distance heat transfer at the inner side is improved, too and in some cases even rewetting can be observed.

1. INTRODUCTION

A precise description of the flow in a curved tube is very difficult due to a secondary flow superimposing on the main flow and even for a single phase fluid the details are not yet known completely. Therefore, post-dryout heat transfer in curved tubes is not only a problem of thermodynamic nonequilibrium but also of very complicated fluiddynamic processes.

Although a considerable number of papers have been published on two phase flow heat transfer in curved and coiled tubes, there have been comparatively few detailed studies of heat transfer, especially in dispersed flow. Correlations only exist for circumferentially averaged heat transfer coefficients, which are mostly evaluated by an analogy to the Lockhart-Martinelli method /1-6/. In these cases the single liquid phase heat transfer coefficient was calculated using the Seban-McLaughlin /7/, Mori-Nakayama /8/ or Rogers-Mayhew /9/ equation. In general, the heat transfer coefficient at the outer side of the bend is higher than that at the inner one (i.e. the side nearer to the bend axis) and the averaged heat transfer coefficient in a curved tube is higher compared to a straight one.

Various investigations have been carried out on critical heat flux in curved tubes /10-14/. The studies have mainly concentrated on the onset of CHF. Some of the findings are summarized in /14/. A more detailed literature review can be found in /15/.

The aim of this present work is the investigation of dispersed flow heat transfer in 90°-tube bends. In the experiments carried out, the dryout does not occur in the bend, but a long distance before the bend inlet. The emphasis of this study is phase separation, that is to say, the transverse motion of the droplets at different mass flowrates and pressures and their influence upon heat transfer. The main differences in dispersed flow between straight and bent tubes are the following:

The slip ratio and the interfacial heat transfer between the phases increase, as the droplets entering the bend move faster towards the outer bend side than the vapour.

Due to the higher radial droplet velocity, the number of droplets impacting on the outer bend wall increase and in case of low wall heat flux rewetting is possible. Whereas droplet-wall contacts are usually neglected in straight tubes, they are of great importance in heat transfer in bent tubes.

In curved tubes the droplet concentration in the cross section is inhomogeneous due to the centrifugal force. Consequently, the extent to which the vapour is superheated depends on the position in the cross section.

The centrifugal force produces a pressure gradient over the cross section of the bent tube with the maximum pressure value on the outer and the minimum on the inner side. In the core of the flow the fluid moves towards the outer side due to the centrifugal force. Close to the wall, where friction prevails, there is an inward flow due to the mentioned pressure difference. By this process a secondary flow consisting of two symmetric vortices is formed (see figure 1).

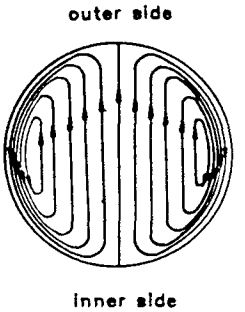

Fig. 1 Streamlines of the secondary flow

2. EXPERIMENTAL APPARATUS

The experiments presented were carried out in a refrigerant R12 loop, which is shown in figure 2. The main components of the loop are a centrifugal pump, a preheater, an evaporator, the test section and a condenser. The test section, mainly consisting of a straight vertical tube and a joint 90°-bend is shown in figure 3. The tube is made of stainless steel with an inner diameter of 28.5 mm. The ratio of bend diameter to tube diameter D/d is 14. The test tube is uniformly heated by direct current. The quality x at the test section inlet is adjusted by the electrically heated evaporator in such a way that the dryout in the vertical tube always occurs about 2.5 m before the bend inlet.

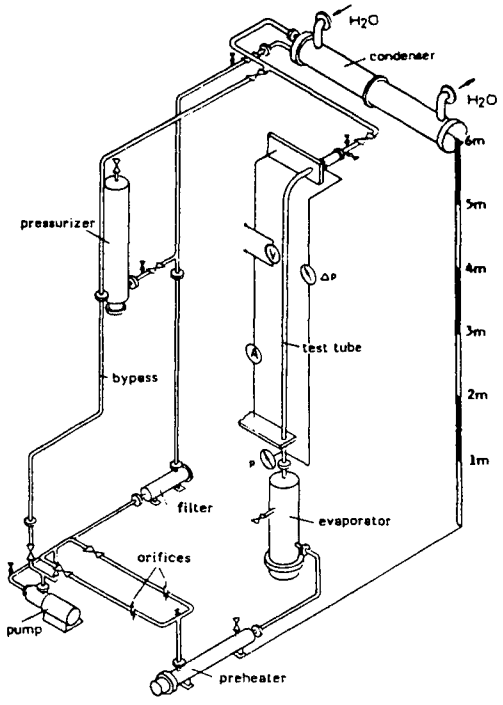

Fig. 2 Test loop

The wall temperatures are measured by 60 chromel-alumel thermocouples (0.5 mm in diameter) which are distributed over the tube length and circumference, as sketched in figure 3.

The vapour temperature is measured in two different ways. On the one hand, we use a vapour probe which utilizes inertial separation of liquid droplets from vapour. It works similar to that of Nijhawan's/16/ shown in figure 4a which consists of two small concentric tubes and one thermocouple in the centre. The sampled fluid which is sucked off from the flow has to transverse through a 180° and a second 90° change in direction before passing over the thermocouple. These directional changes provide the inertial separation of liquid from the vapour. However, droplets impacting on the bottom of the probe and forming a liquid film can move to the top and are sucked off, too. In order to prevent this, we modified our probe as shown in figure 4b. The sampled fluid has only one change in direction before directly streaming into the inner tube. The liquid

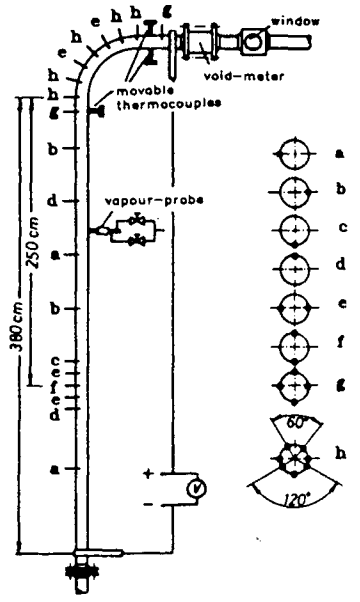

Fig. 3 Test section and distribution of thermocouples

film, however, is sucked off before reaching the top access hole.

On the other hand, we use three bare thermocouples (chromel-alumel, 0.5 mm in diameter), that is to say, thermocouples not shielded from impacting droplets. They are mounted perpendicular to the flow direction before and after the bend and they are movable in the cross section just as the vapour probe. This technique can be employed at high qualities when the time span between two droplets wetting the thermocouple is long enough to allow the thermocouple to dry out again.

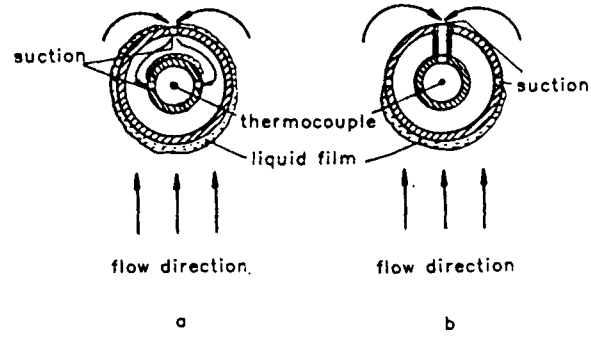

Fig. 4 Vapour probe

Just after the bend outlet a so-called impedance-void-meter is installed. This device is provided for measuring the droplet concentration in different areas of the cross section. Figure 5 shows the device in diameter consisting of concentric tubes, the outer region subdivided in 4 sectors. These tubes are wired to 5 separate capacitors which are supplied with a high frequency voltage. As there is a considerable difference between the permittivities of liquid and vapour, a capacity measurement is a criterion for different void fractions.

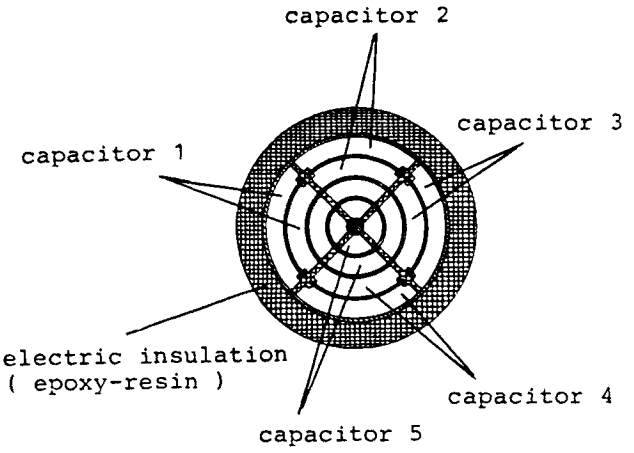

Fig. 5 Impedance-void-meter

3. ANALYSIS OF POST-DRYOUT HEAT TRANSFER

Post-dryout heat transfer in 90°-tube bends is investigated systematically at various mass flux densities (ϕ_m = 400, 680, 1240 and 2000 kg/m²s), reduced pressure ratios ($p/p_{crit} = \pi$ = 0.225, 0.450, 0.675) and wall heat flux densities (q = 2 to 7 W/cm²). The results obtained are discussed in the following section.

3.1. Influence of Fluiddynamic Processes upon Heat Transfer

Typical wall temperature profiles of the inner and outer side of the bend and of the 90°-degree-line are shown in figure 6. The wall temperatures are plotted versus the axial location of the bend, B.I. and A.O. are the positions 10 cm before the bend inlet and 10 cm after the outlet, respectively.

As can be seen by the increasing and decreasing wall temperatures, heat transfer is influenced just at the bend inlet. Obviously the droplets can start moving outwards already a short distance before the inlet. The increase in droplet concentration near the outer wall leads to a reduction in vapour superheat, a better wall heat transfer and lower wall temperatures. The lack of droplets at the inner side effects the opposite. This process is enhanced until a bend angle of about 15 degrees, as can be seen by the steeper wall temperature gradients. Downstream on the outer side the wall temperatures remain nearly unchanged. Why is the wall heat transfer not continuously improved ? On the one hand, a reason is the smaller interfacial heat transfer between the superheated vapour close to the wall and the droplets due to the mentioned decreasing vapour temperature. On the other hand, it is due to the lower droplet mass flow rate reaching the outer wall. The longer the path which the droplets have to follow to the outer wall, the smaller they get in size due to evaporation. Smaller droplets are deflected more easily by the vapour flow and they reach the outer side later, if at all.

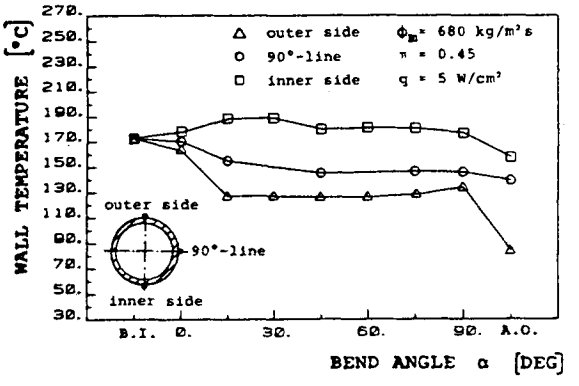

Fig. 6 Wall temperatures at different circumferential locations

On the inner bend side the highest wall temperatures occur at a bend angle of about 15 degrees. Downstream the wall temperatures fall, indicating a similar temperature profile as shown at the outer side and at the 90-degree-line. The example of figure 6 at first shows a slight, then a steep decrease in the wall temperature and from a bend angle of about 45 degrees the temperatures remain nearly unchanged. The improved heat transfer is due to the secondary flow bringing coolant from the outer side. Consequently, changes in the vapour temperature at the outer wall can be detected downstream - in our case about 30 degrees later - at the inner wall. It is very difficult to predict the velocity of the secondary flow by means of the wall temperature, but it seems that within an axial distance of about 30 degrees the secondary flow traverses a circumferential distance of 90 degrees. Under the present geometrical conditions this yields a velocity ratio of the secondary to the main flow of $w_{sf}/w_{mf} \approx 0.2$. At first sight this value seems to be very high, as Patankar /17/ who investigated turbulent single phase flow in 180° bends detected a maximum ratio of only 0.13. A possible explanation for the higher secondary flow velocity is an increase in the circumferential pressure gradient compared with the single phase flow. In dispersed bend flow the droplets stream towards the outer side and evaporate mainly in the superheated vapour close to the outside wall. This yields an additional pressure gradient from the outer to the inner side which accelerates the secondary flow.

3.2. Droplet Trajectories

Heat transfer from the superheated vapour and from the wall to the droplets substantially depends on the droplet trajectories. The radial droplet velocity is a criterion for both the heat transfer between the two phases and the droplet deposition rate at the outer wall. Therefore, trajectories of single drops, entering a 90-degree bend were calculated, not to gain the exact movement of the drops but to assess the influence of different parameters upon the trajectories. Following assumptions were made:

- droplets are spheres and do not evaporate
- axial vapour velocity is constant all over the bend
- slip ratio at the bend inlet is unity
- secondary flow is not taken into account
- thermodynamic properties are constant.

The forces acting on a drop are inertial force, drag force, gravity and buoyancy. The trajectories were calculated numerically with very small time intervals

($\Delta t \leq 1$ msec). The results obtained can be concluded as the following:

An increase in drop size leads to considerably shorter trajectories. The drops are deflected to a lower extent by the vapour flow and strike the outer wall at a smaller bend angle. The relative motion between the two phases increases and so does the Reynolds-number (calculated by the drop diameter and the relative velocity) which is important for the drag coefficient and the interfacial heat transfer.

An increase in the inlet velocity also results in shorter trajectories. However, different inlet velocities do not affect the deflection of droplets as much as different drop diameters.

An increase in the density ratio ρ_v/ρ_l extends the trajectories remarkably. The smaller the difference between the vapour and the liquid density is the stronger is the deflection of the drops by the vapour flow. Though the relative motion decreases, the Reynolds number is nearly unchanged due to the decreasing cinematic viscosity.

3.3. Influence of the Reduced Pressure Ratio p/p_{crit}

Different critical pressure ratios p/p_{crit} do not only influence thermodynamic properties but also flow conditions like quality, flow velocity, drop size etc. Therefore it is difficult to predict how heat transfer is affected.

As illustrated in the above section, drop size and velocity at the bend inlet are very important as to the conditions at the outer wall and heat transfer all over the circumference. Therefore at first the influence of different pressure ratios upon drop size and velocity is assessed.

Droplet velocity. Cumo /18/ found out that in the post-dryout region the slip ratio w_l/w_v is nearly unity. Therefore it is assumed that the velocity of droplets and vapour coincide at the bend inlet.

According to own measurements and correlations predicting the dryout quality x_{DO} the liquid fraction rises with higher pressure ratios. Therefore, with increasing pressures both the vapour density and the mean density of the two phase mixture increase and, consequently - as the mass flux density is constant -the mean flow velocity decreases.

For all experiments carried out the mean velocity at the entrance of the bend was calculated assuming thermodynamic equilibrium. A considerable decrease in velocity is noticed at increasing pressure ratios. For instance, the velocity is reduced by more than 50%, if the pressure ratio increases from 0.225 to 0.45.

Drop size. In the literature some equations predicting the dryout drop size exist, for example /19,20/. The drop sizes calculated by these correlations under the experimental conditions yield an increase in drop diameter with rising pressure ratios. However, Ueda /19/ predicts a much larger increase in drop diameter than Taterson /20/.

In the test tube the dryout point is about 2.5 m before the bend inlet. Therefore, it is to be assessed how drop size changes within this section. Heat transfer from the vapour to the droplets can be calculated by the Benett-eqution /21/

$$h_{vd} = \frac{\lambda f}{d_d} (2 + 0.459\, Re_d^{0.55}\, Pr_f^{0.33}) \quad (1)$$

If the slip ratio is assumed to be unity ($Re_d \rightarrow 0$) and the Spalding-number B considers that the heat transfer coefficient becomes lower than that of a solid sphere due to a vapour layer forming around the drop /22/, the heat flow rate Q_d to a drop can be written as

$$Q_d = h_{vd}\, A\, \Delta T = \pi\, d_d\, 2\, \lambda_f\, \Delta T/(1 + B)^{0.6} \quad (2)$$

The evaporation rate of a drop is

$$\Delta m = Q_d / h_{lv}. \quad (3)$$

From equation (2) and (3) it is evident that with equal temperature difference ΔT the drop-evaporation is stronger at high pressures .On the one hand, the droplet diameter d_d and the thermal conductivity λ_f get larger with increasing pressures which results in a higher heat

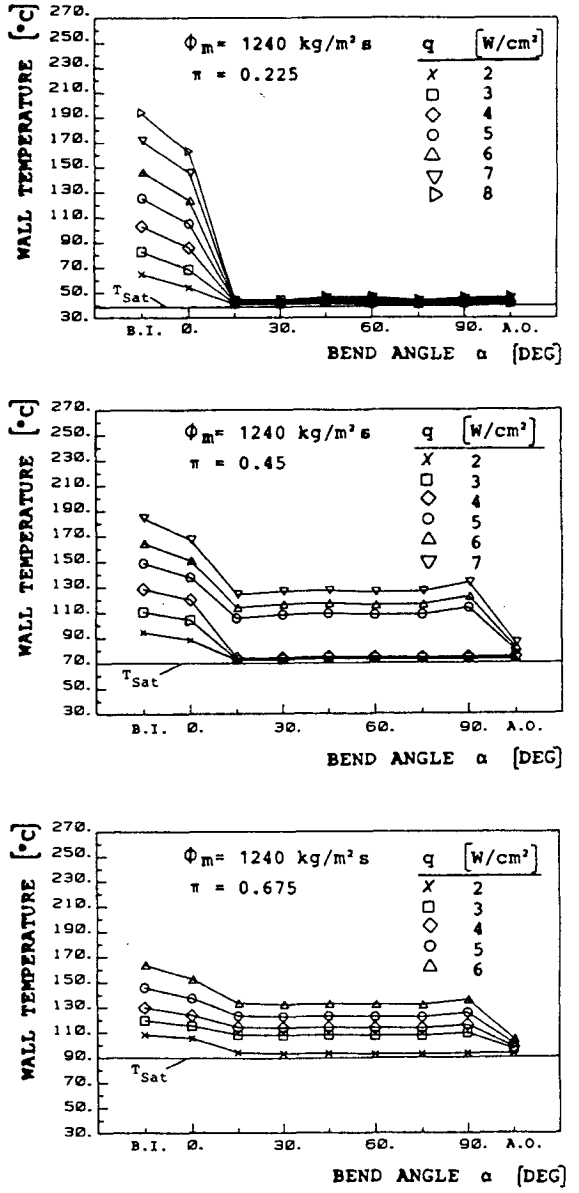

Fig. 7a-c Influence of pressure ratio on wall heat transfer

flow rate Q_d. On the other hand, the heat of evaporation h_{lv} decreases. Moreover, the flow velocity is low at high pressures, as mentioned above, and the period of dwell between the dryout and the bend inlet is longer. Therefore, at high pressure ratios it is possible that the drop size diminishes to the bend inlet to values equal or less than that at low pressure ratios.

Discussion of results. The influence of pressure ratio upon heat transfer is demonstrated in figure 7a - 7c. Data of the outer wall temperature are plotted versus the bend angle at different wall heat flux densities. The wall temperatures generally indicate that rewetting of the outer wall decreases with increasing pressure ratios. Both the heat flux density and the wall temperatures at which rewetting occur decrease. The reason is the lower droplet velocity, the higher drag force of the vapour and probably the smaller drop size which are associated with an increase in pressure ratio. As mentioned above these facts lead to stronger curved droplet trajectories. Furthermore, the force repelling the drops from the wall due to the partial evaporation at that side of the drop facing the heated wall is stronger at high pressures, because of the lower heat of evaporation. Therefore, the droplet velocity perpendicular to the flow direction and the droplet rate reaching the outer wall decrease.

3.4 Influence of Mass Flux Density

The diagrams of figure 8 refer to different mass flux densities. As is well known, in straight tubes higher mass flux densities induce a smaller temperature rise at the dryout point, better heat transfer in the post dryout region and, consequently, lower wall temperatures at a short distance before the bend inlet, as shown in figure 8a and 8b. Moreover, an increase in mass flux density is associated with higher velocities and liquid fractions and smaller drop size. The experimental results illustrate that rewetting at the outer wall is improved and the sector which is rewetted is enlarged by increasing mass flux densities. This is due to the lower wall superheat and higher droplet velocities. The smaller drop size effecting the opposite seems to be of secondary importance in this case.

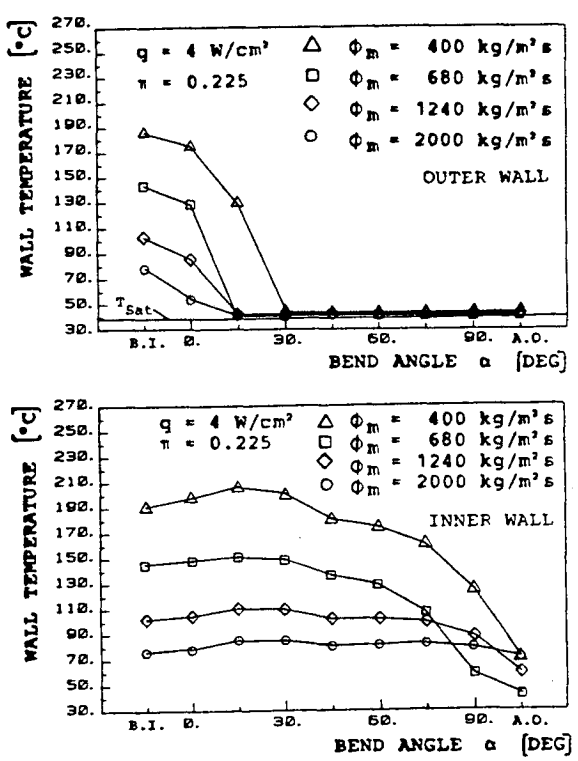

Fig. 8a,b Influence of mass flux density on wall heat transfer

The plots of the wall temperature at the inner side show a decrease in the axial temperature gradient. Partially this is due to the lower wall superheat and vapour temperatures and the resulting less vigorous evaporation of droplets. But there must be another effect, as the wall temperatures at high mass flux densities can even exceed those at low mass flux densities at the bend outlet. Heat transfer at the inner part of the bend mainly depends on the secondary flow. Temperatures at the inner wall begin to fall when coolant from the outer wall reaches this region. An increase in mass flux density leads to rising velocities of the main and secondary flow. If the velocity of the primary flow increases faster than that of the secondary, the inner part of the bend is cooled less and the axial temperature gradient decreases.

3.5 Distribution of Vapour Temperature and Droplet Concentration

For a comparison between correlations of the heat transfer coefficient in the literature and own measurements the actual vapour temperature near the wall and its change from the bend inlet to the outlet is required. This mainly depends on the droplet distribution in the cross section. Therefore, both the vapour temperature and the droplet concentration are measured at different locations in the cross section just after the bend outlet.

From figure 9 showing a typical plot of vapour superheat at different pressure ratios two tendencies can be seen. Firstly, the extent to which vapour is superheated increases as the pressure ratio decreases. Secondly, the region in which vapour is superheated extends from the inner towards the outer wall with decreasing pressure ratios.

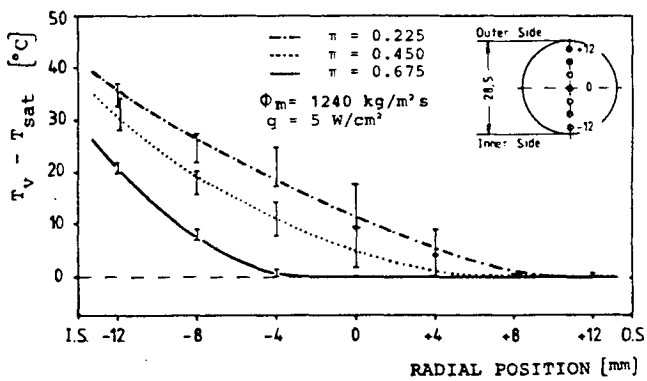

Fig. 9 Distribution of vapour temperature in the cross section

The data of figure 10 obtained by the impedance-void-meter show the distribution of droplets in the cross section. In the region close to the inner wall (3) the void fraction nearly coincides with the value of pure vapour phase. In the core of the cross section (2) the liquid fraction is little higher but low compared to the outer region (1) in which the predominant part of the droplets flow. A comparison between figure 10a and 10b demonstrates that the impedance-void-meter is very sensitive and of fast response. It clearly detects how the fluctuations in droplet concentration and the droplet distribution is influenced if the averaged void fraction is changed.

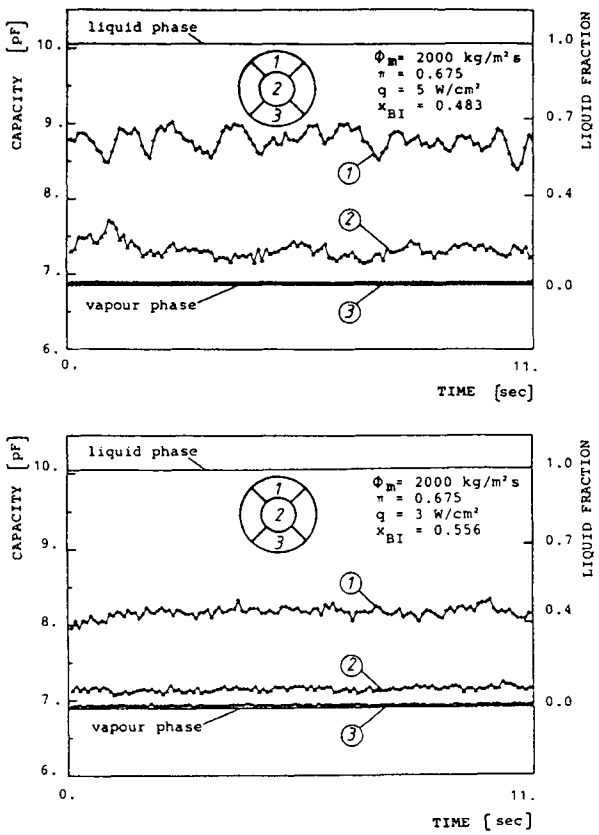

Fig. 10a,b Distribution of liquid fraction in the cross section

ACKNOWLEDGEMENT

The author wishes to thank the Deutsche Forschungsgemeinschaft (DFG) which supported this work.

REFERENCES

1. Owhadi,A., Boiling in Self-Induced Radial Acceleration Fields, Ph.D. Thesis, Oklahoma State University, Stillwater, 1966
2. Owhadi,A., Bell,K.J., Forced Convection Boiling Inside Helically-Coiled Tubes, Int. J. Heat Mass Transfer 11: pp 1779-1793, 1968
3. Kozeki,M., Boiling Heat Transfer in Curved Tube, Mitsui Shipbuilding and Engineering Co, Tokyo, Japan
4. La Harpe,A., Lahongre,S., Mollard,J., Johannes C., Boiling Heat Transfer and Pressure Drop of Liquid Helium Under Forced Circul. in a Helic. Coiled Tube, Adv. in Cryog. Eng. 14, 1969
5. Kozeki M., Film Thickness and Flow Boiling for Two Phase Annular Flow in a Helically Coiled Tube, Proc. Int. Meeting on Reactor Heat Transfer, Ges. f. Reaktorf., Karlsruhe, 1973
6. Crain B., Jr., Bell K.J., Forced Convection Heat Transfer to a Two-Phase -Mixture of Water and Steam in a Helical Coil, AIChE Symposium Series No 13169: pp 30-36, 1973
7. Seban,R.A., McLaughlin,E.F., Heat Transfer in Tube Coils with Laminar and Turbulent Flow, Int. J. Heat Mass Transfer 6, pp 387-395, 1963
8. Mori,Y., Nakayama,W., Study on Forced Convection Heat Transfer in Curved Pipes (Second Report, Turbulent Region), Int. J. Heat Mass Transfer 10, pp 37-59, 1967
9. Rogers,G.F.,Mayew,Y.R., Heat Transfer and Pressure Loss in Helically Coiled Tubes with Turbulent Flow, Int.J. Heat Mass Transfer 7, pp 1207-1216, 1964
10. Carver,J.R., Kakarala,C.R., Slotuik,J.S., Heat Transfer in Coiled Tubes in Two Phase Flow, Babcock and Wilson Comp. Res. Rep. 4438, 1964
11. Miropolskiy,Z.L.,Picus,V.J.,Shitsman,M.E., Regimes of Deteriorated Heat Transfer at Forced Flow of Fluids in Curvilinear Channels, Proc. 3rd Int. Heat Transfer Conf., Chicago, Vol 2, pp 97-101, AIChE, 1966
12. Barbarin V.P., Sevasty'yanov,R.I., Alad'yev,I.T., Khudyakov,V.F., Tzachev,V.A., CHF in Tubular Coils, Heat-Transfer-Soviet Res. 3, No 4, 1971, 85-90
13. Cumo,M., Farello,G.E., Ferrari,G., The Influence of Curvature in Post-Dryout Heat Transfer, Int. J. Heat Mass Transfer 15, pp 2045-2062, 1972
14. Jensen,M.K., Bergles,A.E., CHF in Helically Coiled Tubes, Transact. ASME, J.of Heat Transfer, Vol 103, pp 660-666, 1981
15. Jensen,M.K., Boiling Heat Transfer and CHF in Helical Coils, Ph.D. Thesis, Iowa State University, 1980
16. Nijhawan,S., Chen,J.C., Sunderam,R.K., London, E.J., Measurements of Vapour Superheat in Post-Critical-Heatflux boiling, Trans. ASME, J. of Heat Transfer, Vol 102, pp 465-470, 1980
17. Patankar,S.V., Pratap,V.S., Spalding,D.B., Prediction of Turbulent Flow in Curved Pipes, J. Fluid Mech., Vol 67, part 3, pp 583-595, 1975
18. Cumo,M., Ferrari,G., Farello,G.E., A Photogr. Study of Two Phase, Liquid Dispersed Flows, Rep. XXV Nat. ATI Annual Meeting, 1971
19. Ueda,T., Tanaka,H., Koizumi,Y., Dryout of Liqid Film in High Quality R-113 Upflow in a Heated Tube, Proc. 6th Int. Heat Transfer Conf., Toronto, 1978
20. Tatterson,D.F.,Dallman,J.C.,Henratty,T.J., Drop Size in Annular Gas-Liquid Flows, AIChE Journal 23, 1977
21. Bennett,A.W.,Hewitt,G.F.,Kearsey,H.A.,Keeys,R.K.F., Heat Transfer to Steam Water Mixtures Flowing in Uniformly Heated Tubes in which the CHF has been Exceeded, UKAEA Rep. AERE-R5373, 1967
22. Hofman,T.W., Ross,L.L., A Theoret. Invest. of the Effect of Mass Transfer on Heat Transfer to an Evaporating Droplet, Int. J. Heat Mass Transfer 15, pp 599-617, 1972